GeoStudio Example File
Factors Controlling Rainfall-Induced Instability

To see the latest GeoStudio learning content, visit Seequent Learning Centre and search the catalogue for “GeoStudio”.

Introduction

It is well known that infiltration can destabilize man-made or natural slopes. Rainfall-induced slope failures are reported to occur during, or immediately after, periods of intense, or low-intensity but long-duration, rainfall (Tan et al., 1987; Anderson and Zhu, 1996; Rahardjo, 2000; Ng et al., 2001). There are a number of factors that govern stability during rainfall including slope geometry, soil properties, rainfall intensity and duration, antecedent moisture conditions, and the location of the initial water table. The objective of this example is to highlight the relative importance of some of these factors on the stability of predominately unsaturated slopes.

Background

Shear Strength of Unsaturated Soil

There are a number of equations available in the literature to describe the shear strength of unsaturated soils. Fredlund et al. (1978) proposed a linear relationship that is written as:

$$\tau = c^{'} + (\sigma_n - u_a)tan\phi^{'} + (u_a - u_w)tan\phi^b$$ **Equation 1**

where τ is the shear strength, $c^{'}$ the effective cohesion, $(\sigma_n - u_a)$ the net normal stress on the failure plane, σ_n the total normal stress; u_a the air pore-air pressure; u_w the pore-water pressure; $(u_a - u_w)$ the matric suction; $\phi^{'}$ the friction angle; and, ϕ^b the angle linking the rate of increase in shear strength with increasing matric suction. Vanapalli et al. (1996) suggested a non-linear shear strength equation that involved a normalization of the volumetric water content function given by:

$$\tau = c^{'} + (\sigma_n - u_a)tan\phi^{'} + (u_a - u_w)S_e tan\varphi^{'}$$ **Equation 2**

where S_e is the effective degree of saturation given by:

$$S_e = \frac{\theta - \theta_r}{\theta_s - \theta_r}$$ **Equation 3**

where θ is the volumetric water content and the subscripts r and s indicate residul and saturation, respectively. The non-linear strength equation provides a better representation of unsaturated soil behavior. The literature clearly demonstrates that the unsaturated shear strength can be related to the volumetric water content function. According to Equation 2 and Equation 3, the shear strength of an unsaturated soil increases nearly proportionally with matric suction until the air entry value is reached. At higher matric suctions, the suction strength decreases non-linearly, and in accordance with the decrease in effective degree of saturation, reaching zero once the volumetric water content is equal to the residual value (i.e. θ = θ_r). The relationship between suction strength and matric suction is soil type dependent via the relationship between volumetric water content and matric suction.

Infiltration into Unsaturated Soils

The propagation of a wetting front into an unsaturated soil is governed by the infiltration flux (q) and the hydraulic conductivity (K) function of the soil. Figure 1 presents illustrative pore-water pressure profiles at two successive times once the flux on the ground surface returns to an annual average value after a rainfall event. The rainfall and average annual fluxes are both less than the saturated hydraulic conductivity K_s of the soil. As noted by Kisch (1959), the pore-water pressure head gradient becomes zero behind the wetting front, which is reflected in the vertical portion of the pore-water pressure profile, resulting in a total hydraulic head gradient (i) that is equal to 1.0. The pore-water pressure behind the wetting front corresponds to an unsaturated hydraulic conductivity that just large enough to support the average infiltration flux; that is, the hydraulic conductivity is equal to the background flux. The negative pore-water pressure behind the wetting front can therefore be anticipated by looking up the value corresponding to $q = K$ from the hydraulic conductivity function (Figure 2).

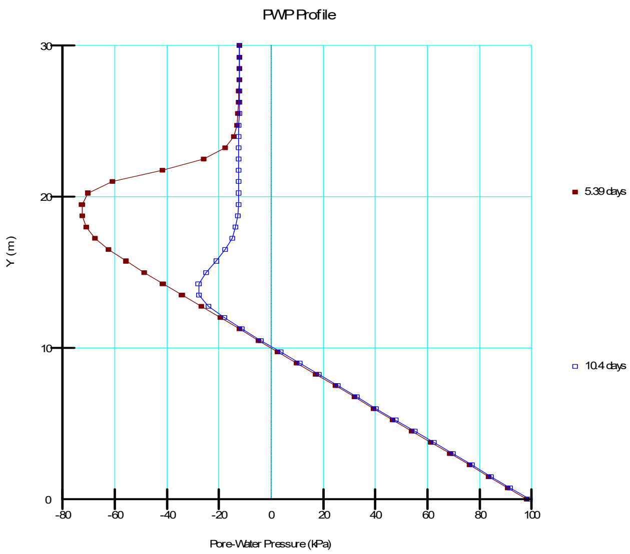

Figure 1. Pore-water pressure profile for a transient infiltration analysis.

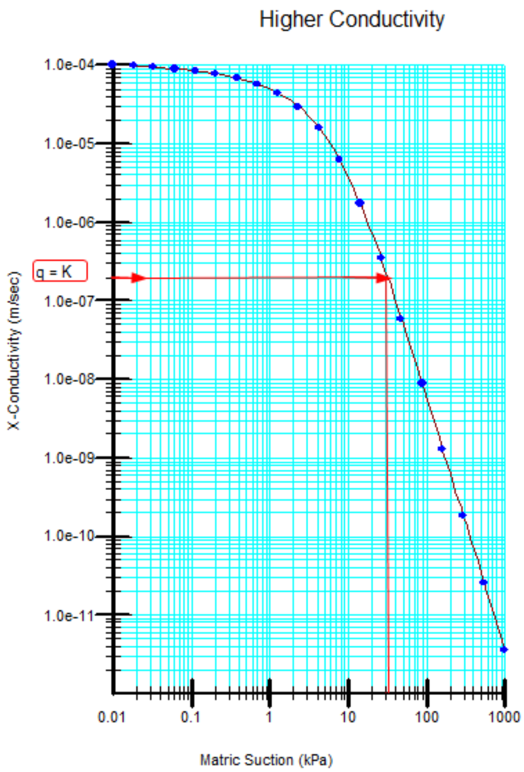

Figure 2. Determining pore-water pressure for infiltration flux < Ks.

Numerical Simulation

Rahardjo et al. (2007) conducted a parametric study involving eighty-four combinations of soil type, slope angle, rainfall intensity, slope height, and groundwater table depth. The parametric study completed for this examples gives consideration to material properties, rainfall intensity, and antecedent moisture condition. In engineering practice, the slope geometry must naturally be considered given that that the factor of safety (FOS) decreases as slope height and angle increase (Rahardjo et al., 2007), making the effect of rainfall on stability more pronounced. The initial water table depth does influence antecedent moisture conditions, but Wong and Ho (1998) found that only 2% of slope failures in Hong Kong could be attributed to a rise in the water table.

Figure 3 presents the model configuration and hydraulic boundary conditions. The slope angle is assumed to be approximately 40° based on the work of Toll et al. (1999) who suggested that thirty-five failed slopes in Singapore had slope angles greater than 27° and less than 70°. The slope height is 10 m. The shear strength parameters for the soil were assumed to be c' = 2 kPa, ϕ' = 26°, and the soil unit weight equal to 20 kN/m^3 (refer to the associated GSZ project file).

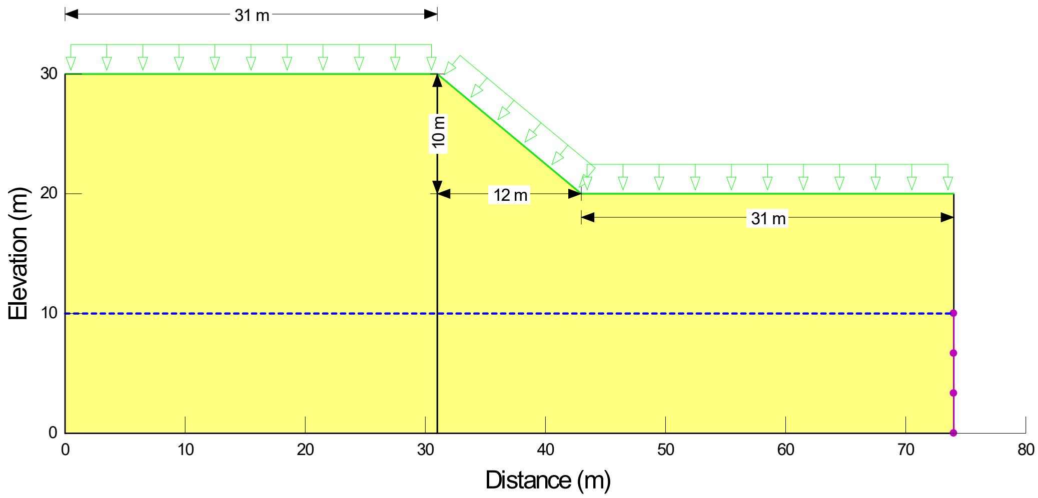

Figure 3. Model Geometry and boundary conditions.

Figure 4 presents the Analysis Tree for the GeoStudio Project. The pore-water pressure distribution for each SLOPE/W analysis is defined by its Parent steady-state or transient SEEP/W analysis. In the case that a transient analysis is the Parent, the pore-water pressure definition in the Child SLOPE/W analysis is set to 'all', meaning the FOS is calculated at every saved time step (Figure 5). A total of six cases, each case comprising a number of scenarios described subsequently, were analyzed. Cases 1 to 4 were developed to investigate the effect of rainfall intensity and soil properties on the FOS. Case 5 and Case 6 were developed to investigate the effect of antecedent moisture conditions on long-term stability.

Analyses
- Case 1 - low K and 9 mm/hr
  - 1a - Initial FOS without Suction Strength
  - 1b - Initial FOS with Phi B
  - 1c - Initial FOS with VWC Suction St.
  - 1d - FOS During Infil.with Phi B
  - 1e - FOS During Infil. with VWC Suction St.
- Case 2 - high K and 9 mm/hr
  - 2a - Initial FOS without Suction Strength
  - 2b - Initial FOS with Phi B
  - 2c - Initial FOS with VWC Suction St.
  - 2d - FOS During Infil.with Phi B
  - 2e -FOS During Infil. with VWC Suction St.
- Case 3 - low K and 80 mm/hr
  - 3a - FOS During Infil.with Phi B
  - 3b - FOS During Infil. with VWC Suction St.
- Case 4 - high K and 80 mm/hr
  - 4a - FOS During Infil.with Phi B
  - 4b -FOS During Infil. with VWC Suction St.
- Case 5 - low K and 1 m/yr
  - 5a - FOS with VWC Suction St.
- Case 6 - high K and 1 m/yr
  - 6a - FOS with VWC Suction St.

Figure 4. Analysis Tree for the GeoStudio Project.

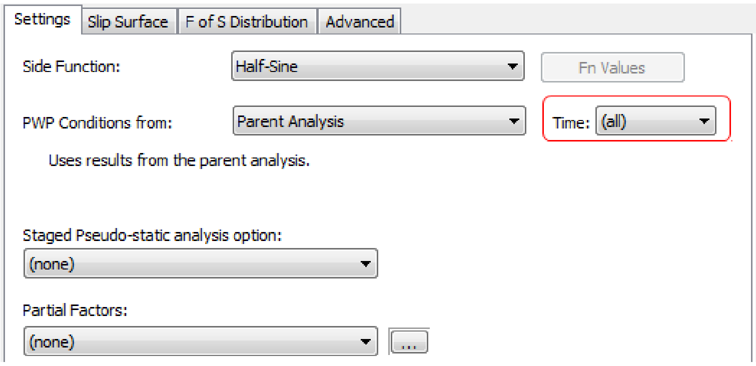

Figure 5. Pore-water pressure definition for determining FOS from a transient SEEP/W analysis.

Case 1 and 2 compare the response of the low K and high K soils to a low intensity rainfall of 9 mm/hr and each comprise five stability analyses. The analyses labeled “a” calculate the FOS without suction strength prior to rainfall. The analyses labeled “b” and “c” calculate the FOS prior to rainfall and include suction strength as per the last terms in Equation 1 and Equation 2, respectively. The analyses labeled “d” and “e” calculate the FOS during the rainfall event and include suction strength as per the last terms in Equation 1 and Equation 2, respectively.

Case 3 and 4 compare the response of the low K and high K soils to a high intensity rainfall of 80 mm/hr. The analyses labeled “a” and “b” calculate the FOS during the rainfall event and include suction strength as per the last terms in Equation 1 and Equation 2, respectively. These two analyses are similar to “d” and “e” of Case 1, except that the infiltration flux is much higher.

Case 5 and 6 compare the long-term stability of the low K and high K soils to a steady-state annual average infiltration flux of 1 m/yr. The analyses labeled “a” calculate the FOS and include suction strength as per the last terms in Equation 2.

The suction strength parameter (ϕ^b) for scenarios involving the Equation 1 was set to 20° (Rahardjo et al., 2007). As will be demonstrated, the use of a linear unsaturated strength law, combined with a ϕ^b that gives no consideration to soil type or volumetric water content, can be misleading. The suction strength at the base of slices for scenarios involving Equation 2 is calculated by the solver.

Transient groundwater flow analyses require an initial condition. An initial water table with a maximum negative pressure head equal to 7.5 m (~ 75 kPa) was used to define the initial conditions in Cases 1 through 4, which is consistent with Rahardjo et al. (2007). In the physical reality, the initial condition for soil profiles comprising different materials – in this study the low K and high K materials - should be different. This aspect of the parametric study is explored by means of the the steady-state ground water flow analyses for Case 5 and 6.

The rainfall event and average annual infiltration flux were represented by a water flux verses time boundary condition and a constant flux boundary condition, respectively. A total head of 10 m was assigned to the right of the model domain. The left and bottom sides of the domain are no-flow boundaries (Figure 3). The total duration of each transient seepage analysis was 5 days. The duration of the rainfall event was assumed to be 24 hours (refer to the associated GSZ project file).

The hydraulic conductivity and volumetric water content functions for the SEEP/W analyses were estimated using the van Genuchten input parameters shown in Table 1. The two soils were designated as ‘low conductivity’ and ‘high conductivity’ based on the saturated hydraulic conductivity K_s values of 1e-6 m/s and 1e-4 m/s, respectively. Figure 6 shows the estimated volumetric water content functions for both materials.

Table 1. van Genuchten Input Parameters

Material	K_s (m/s)	α (kPa)	n	θs	θr
Low K	1e-6	100	1.5	0.45	0.45
High K	1e-4	10	1.5	0.05	0.05

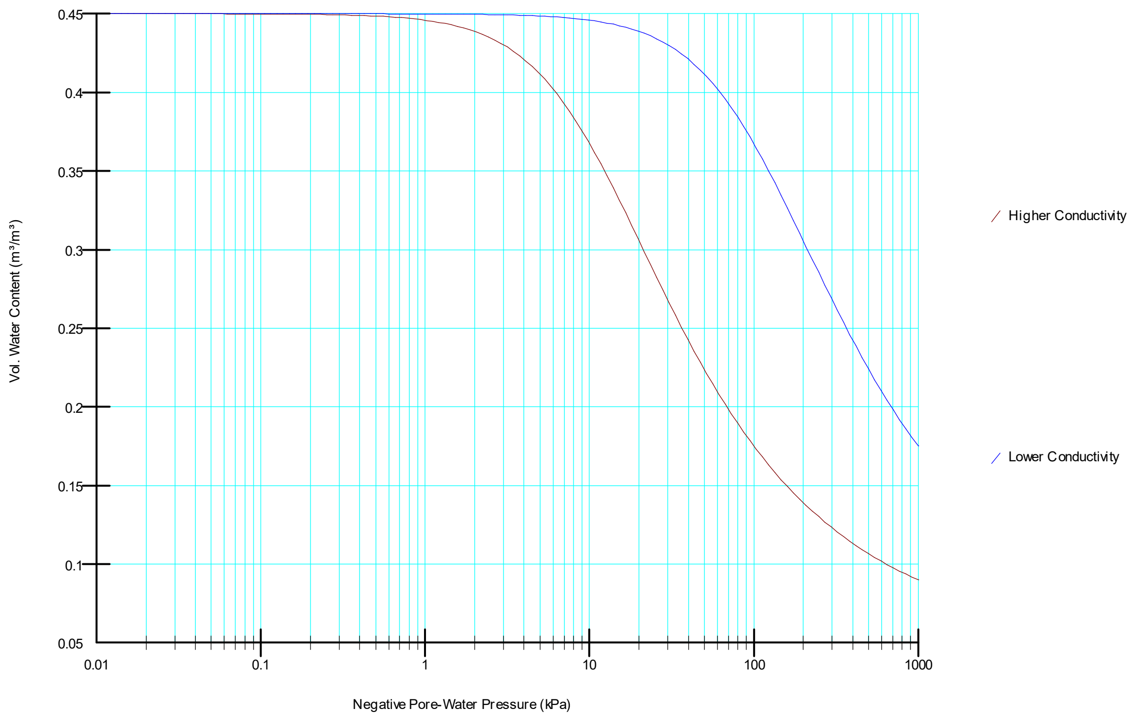

Figure 6. Volumetric water content functions for the material properties shown in Table 1.

Figure 7 shows the suction strengths, calculated independently in a spreadsheet, for the low K and high K materials over a large matric suction range. The suction strengths were calculated from last term in Equation 2. The effective degree of saturation (Equation 3) was calculated from the data the defines the volumetric water content functions shown in Figure 6. The plots reveal the non-linearity on the strength equation and the role of water holding capacity – that is, the 'texture' of the soil – to generate suction strengths at high matric suctions. Clearly the low K material retains more water at higher suctions (Figure 6), resulting in a higher S_e and therefore a higher suction strength.

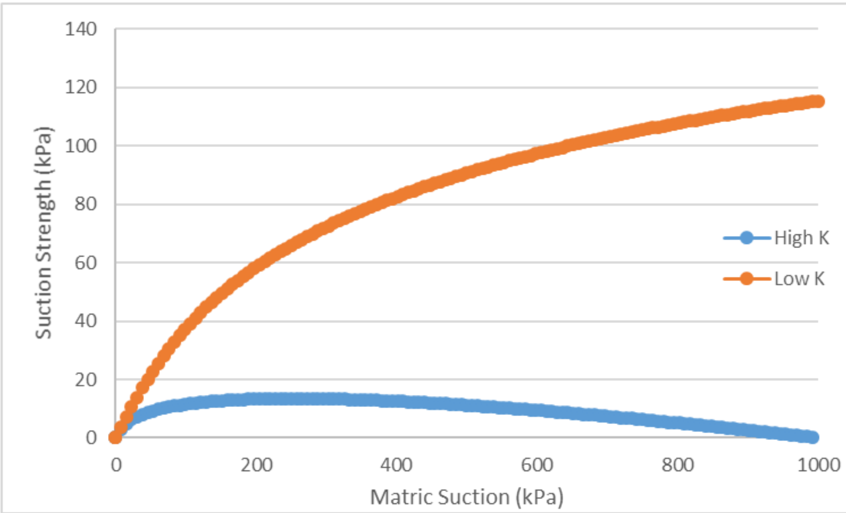

Figure 7. Suction strength calculated from last term in Equation 2, Equation 3, and the volumetric water content functions shown in Figure 6.

Results and Discussion

Stability Prior to Rainfall

Figure 8 and Figure 9 present the stability results prior to rainfall for the cases that exclude suction strength (Case 1a and 2a) and that include suction strength calculated by Equation 1 (Case 1b and 2b), respectively. The FOS prior to rainfall is the same for the lower K and higher K soils when suction is excluded (Figure 8) because both materials have the same friction angle, ϕ', cohesion, and unit weight. Similarly, Case 1b and 2b yield the same FOS because Equation 1 is linear; meaning that the effects of the antecedent volumetric water content distribution on suction strength is independent of soil type. Regardless of the deficiencies associated with Equation 1, a comparison of Figure 8 and Figure 9 reveals that the slope would not be stable before a rainfall event unless suction strength is considered.

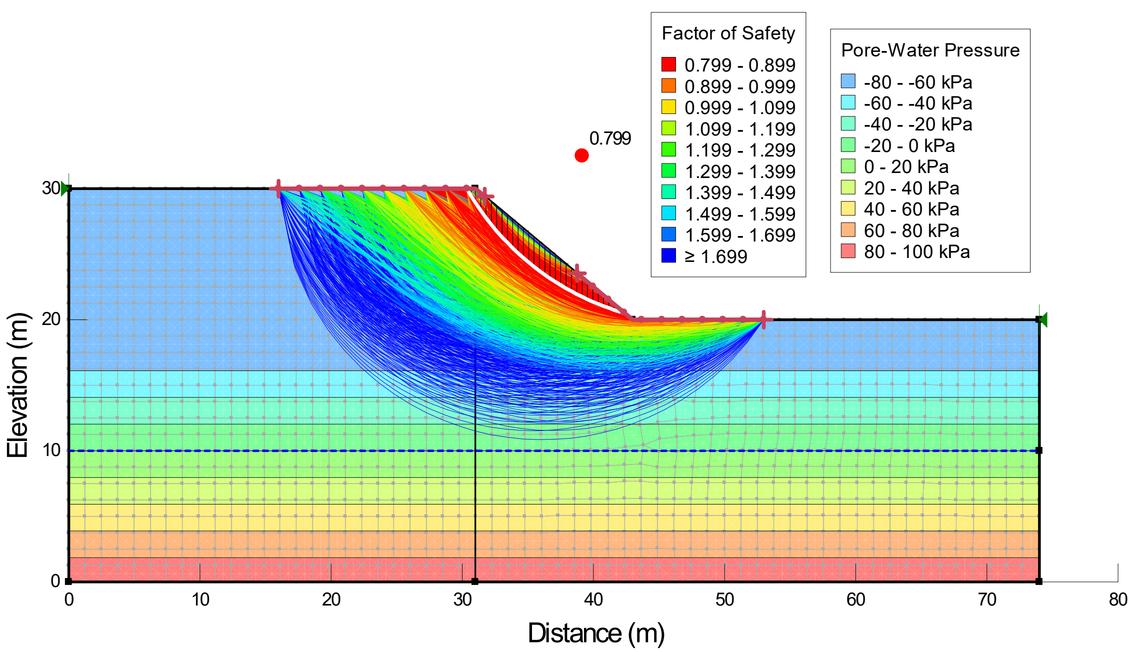

Figure 8. FOS prior to rainfall when suction strength is excluded for Case 1a and 2a.

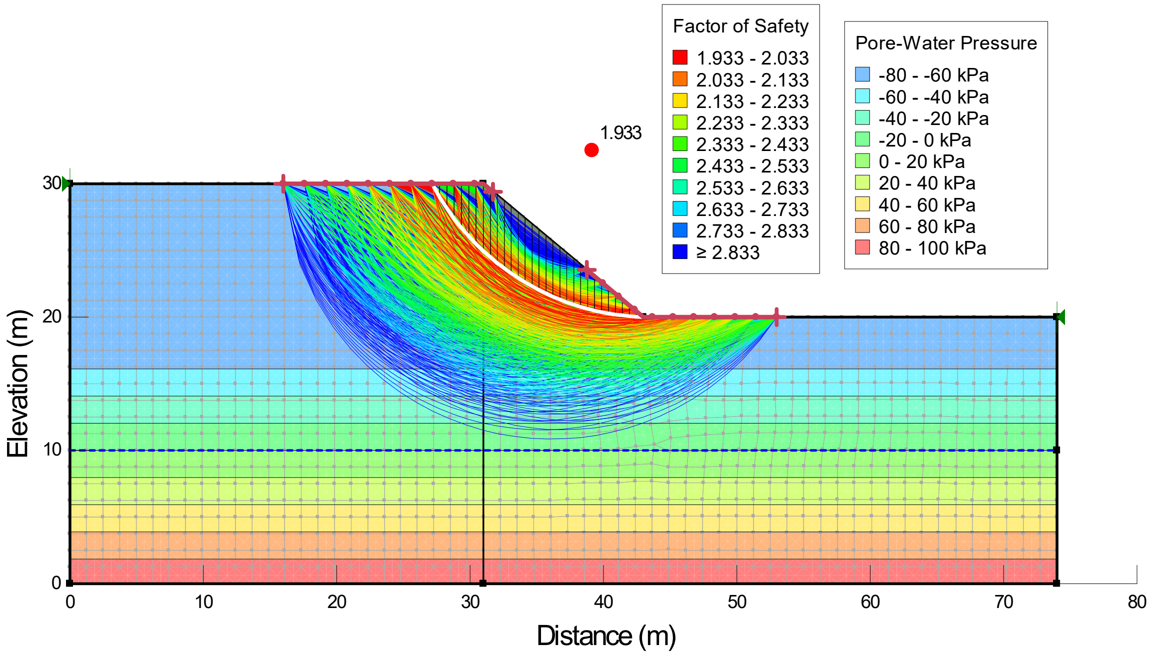

Figure 9. FOS prior to rainfall using linear suction strength definition (ϕ_b) for Case 1b and 2b.

Figure 10 and Figure 11 compare the FOS prior to rainfall when the suction strength is defined using Equation 2 for the low K and high K soil, respectively (Case 1c and 2c). In contrast to Case 1b and 2b, the FOS prior to rainfall is different between these two cases because the suction shear strength relationship is non-linear and soil type dependent. The initial pore-water pressure along the base of the critical slip is about -75 kPa for both cases, resulting in a suction strength of about 30 kPa and 10.5 kPa for the low K and high K materials, respectively (Figure 7). The Low K material's water retention capacity at higher matric suctions has a significant effect on the FOS prior to the rainfall event.

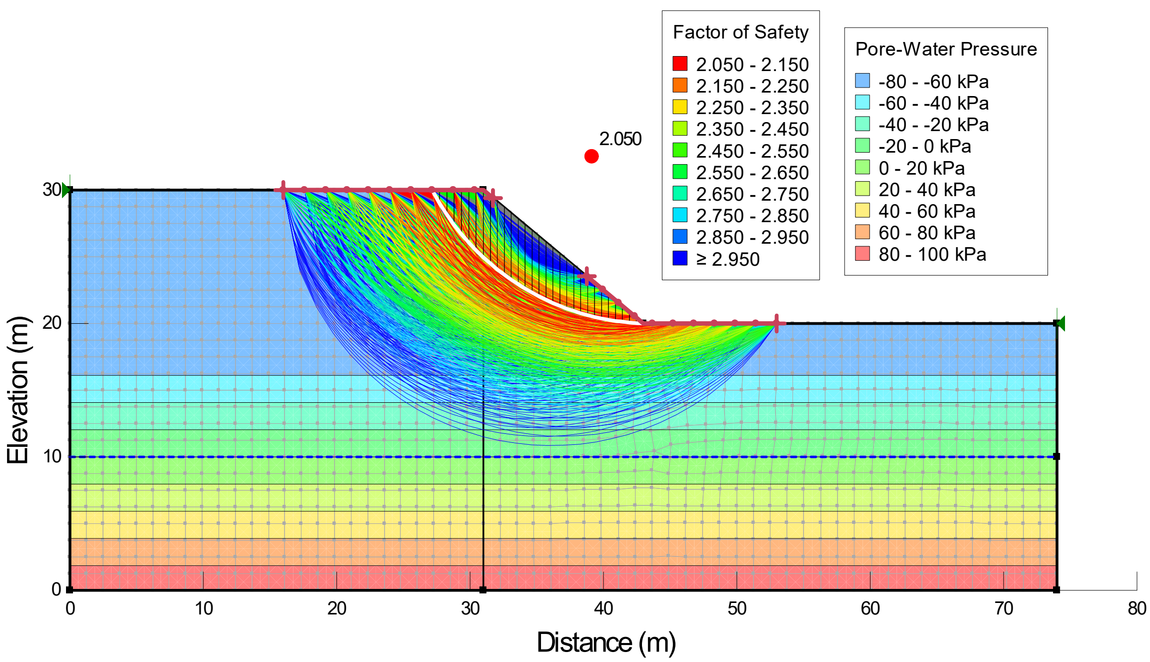

Figure 10. FOS Prior to Rainfall for the Lower K Material using VWC Suction Strength (Case 1c).

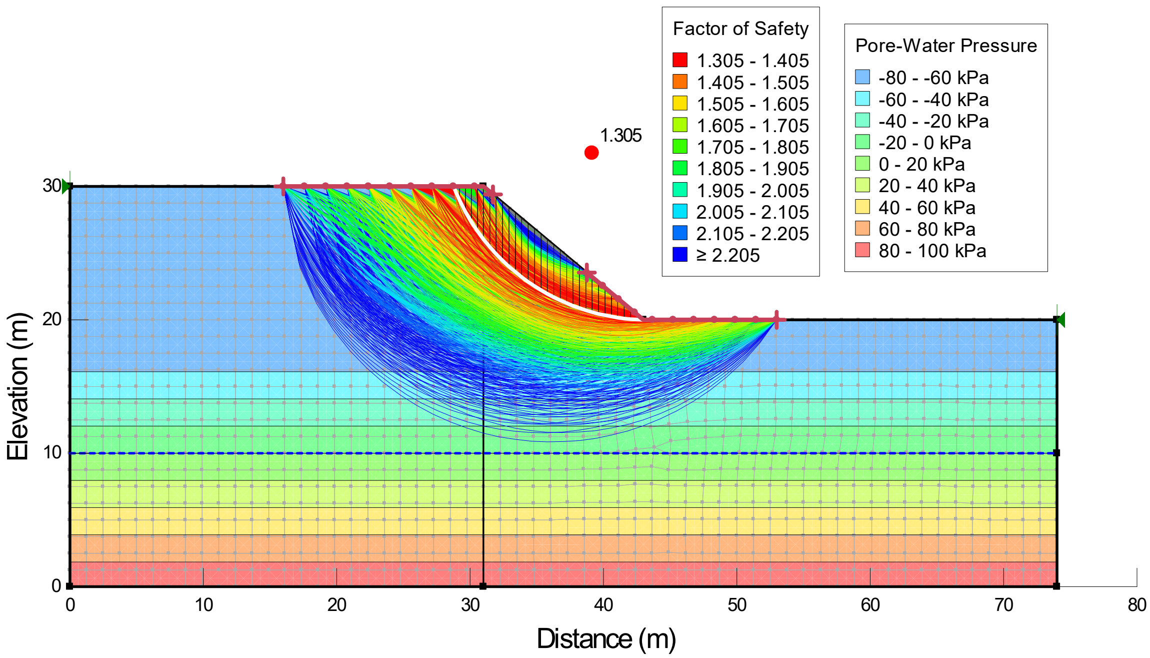

Figure 11. FOS Prior to Rainfall for the Higher K Material using VWC Suction Strength (Case 2c).

Rainfall Intensity and Soil Properties

Figure 12 (Case 1d/2d) and Figure 13 (Case 3a/4a) present the FOS verses time for the 9 mm/hr and 80 mm/hr rainfall events, respectively, and the suction strength defined by Equation 1. As has already been demonstrated, the use of the same ϕ^b for both materials is nonsensical. Regardless, a comparison of Figure 12 and Figure 13 is instructive because any differences in the FOS response are due solely to changes in matric suction. The reduction in FOS is more precipitous and larger for the lower K soil than the higher K soil when the rainfall flux is 9 mm/hr (Figure 12). In contrast, the opposite is true for the 80 mm/hr rainfall (Figure 13): the drop in FOS is more dramatic for the higher K soil.

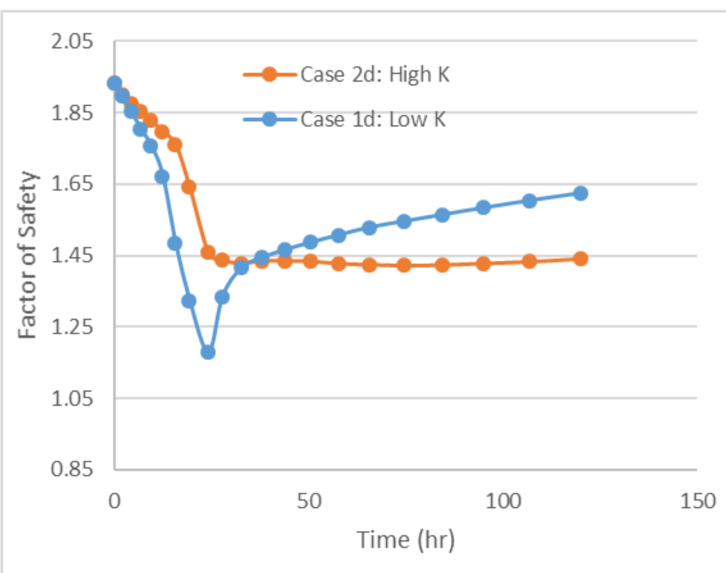

Figure 12. Comparison of FOS for a Rainfall Flux of 9 mm/hr using Phi B .

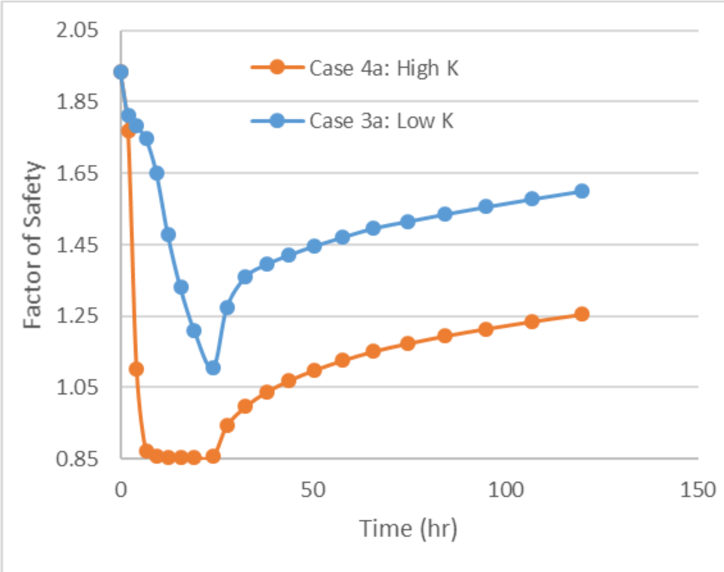

Figure 13. Comparison of FOS for a Rainfall Flux of 80 mm/hr using Phi B.

Figure 14 presents the pore-water pressure profile after 24 hours with a rainfall flux of 9 mm/hr. Figure 15 presents the pore-water pressure profile after 24 hours with a rainfall flux of 80 mm/hr. Figure 16 presents the hydraulic conductivity functions relative to the infiltration fluxes.

An infiltration flux of 9 mm/hr is greater than K_s of the low K soil but easily accommodated by the high K soil in an unsaturated state (Figure 16). Runoff is initiated after about 6.5 hours in the low K soil, causing the pore-water pressure to be zero at the ground surface (Figure 14). In contrast, the infiltration flux of 9 mm/hr is much less than K_s for the high K soil, so the pore-water pressure at the ground surface does not tend toward zero. The loss of matric suction (i.e. increase in pore-water pressure) is therefore greater in the low K soil, causing the factor of safety reduction to be greater compared to the higher K soil (Figure 12). Again, it is important to recall that the suction strength calculated by Equation 1 is independent of material type and ϕ^b was assumed the same for both soils. The only factor controlling suction strength is the change in matric suction; the soil profile with the largest decrease in matric suction will experience the most significant decrease in factor of safety.

Having stated this, an infiltration flux of 80 mm/hr is much greater than the K_s of the low K soil but still below the K_s of the high K soil (Figure 16). The wetting front propagates much deeper into the soil profile for the high K soil (Figure 15), resulting in a significant increase in matric suction and therefore loss of suction strength and decrease in FOS (Figure 13). The pore-water pressure profile is vertical behind the wetting front and has a value of about -3 kPa, which corresponds to $q = K = 80$ mm/hr for the high K soil (Figure 16). The pore-water pressure profile for the lower K soil, however, is not much different than shown in Figure 14 given that the infiltration flux is much greater than K_s and the pore-water pressure at the ground surface goes to zero near the onset of rainfall.

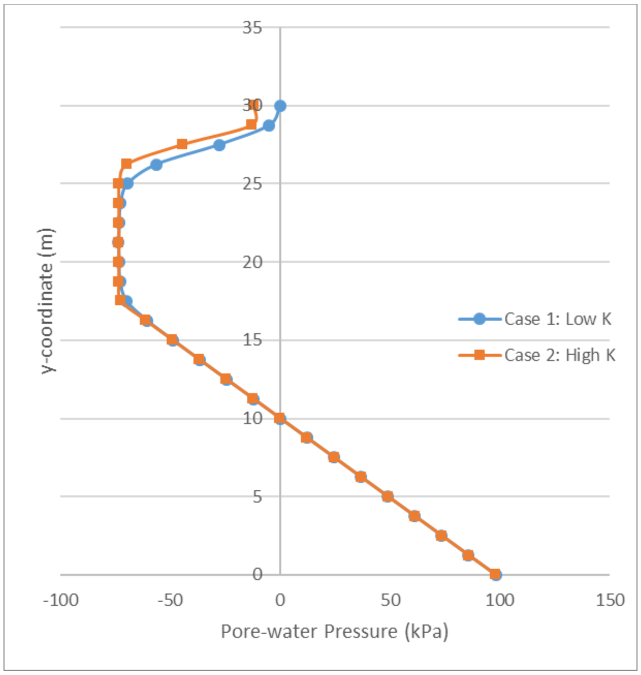

Figure 14. Pore-water pressure profiles during 9 mm/hr rainfall event after 24 hours.

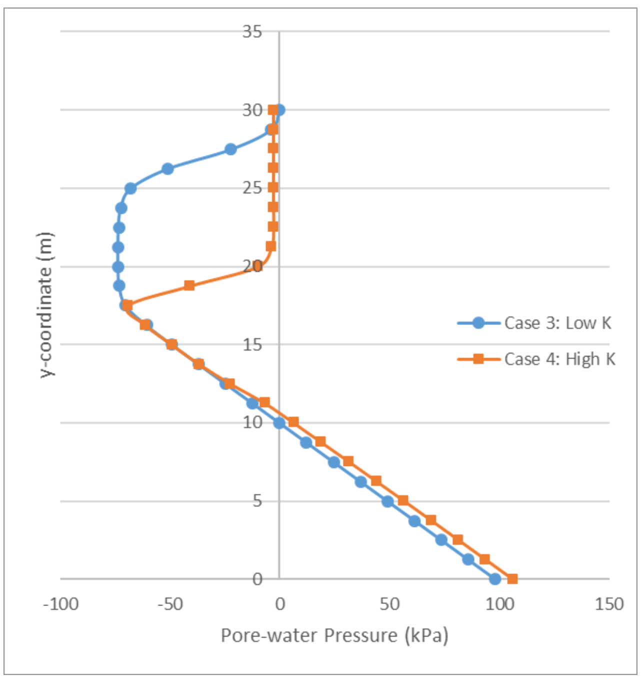

Figure 15. Pore-water pressure profiles during 80 mm/hr rainfall event after 24 hours.

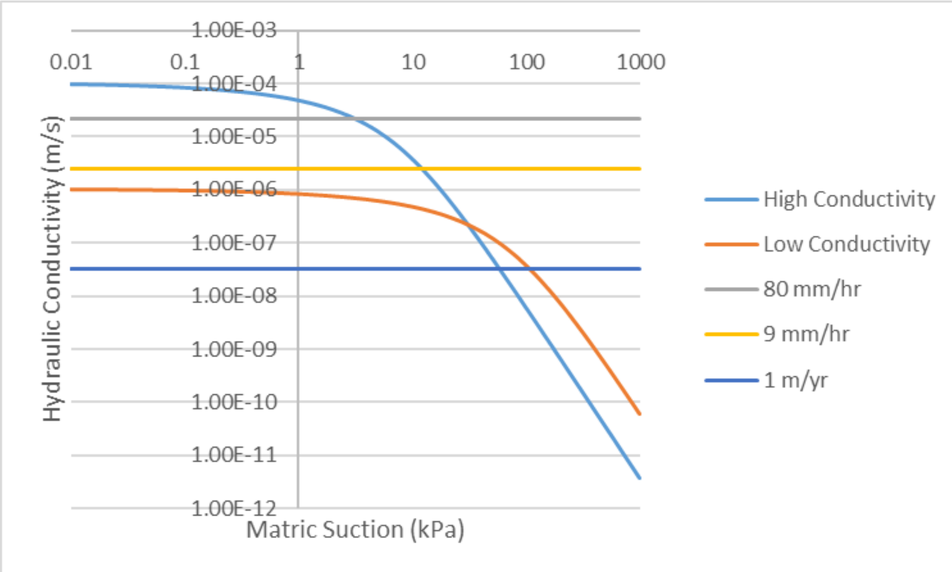

Figure 16. Hydraulic conductivity functions relative to rainfall fluxes of 9 mm/hr, 80 mm/hr, and 1 m/yr.

Importance of Non-Linear Suction Strength

Figure 17 and Figure 18 present the minimum FOS verses time for the 9 mm/hr and 80 mm/hr rainfall intensities when the non-linear suction strength definition is used. As noted above, the FOS prior to rainfall is substantially lower for the higher K soil because it does not generate as much suction strength for the same pore-water pressure distribution. As the wetting front propagates, both soils experience a drop in FOS, but the drop is more dramatic for the lower K soil because it starts with a greater suction strength. The higher K soil does not reach a state of failure for the 9 mm/hr rainfall intensity, but the FOS does drop below 1.0 for the 80 mm/hr rainfall because of the rapid descent of the wetting front and corresponding decrease in S_e (Equation 3).

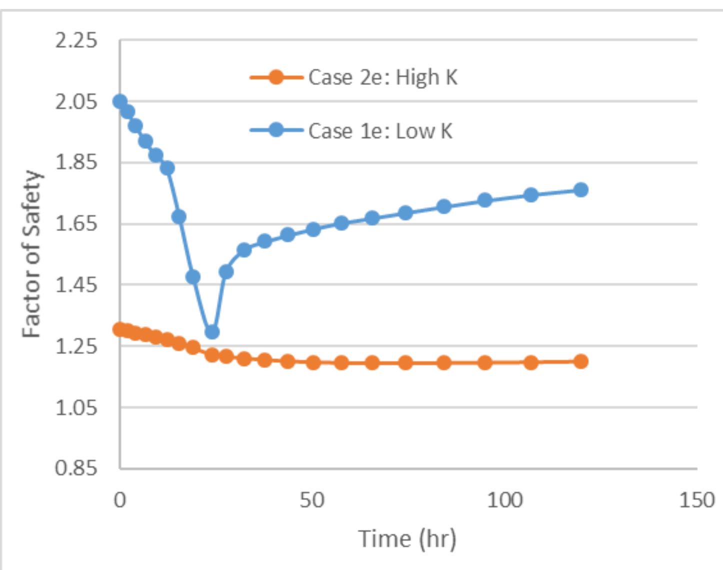

Figure 17. Comparison of FOS for a Rainfall Flux of 9 mm/hr using VWC Suction Strength.

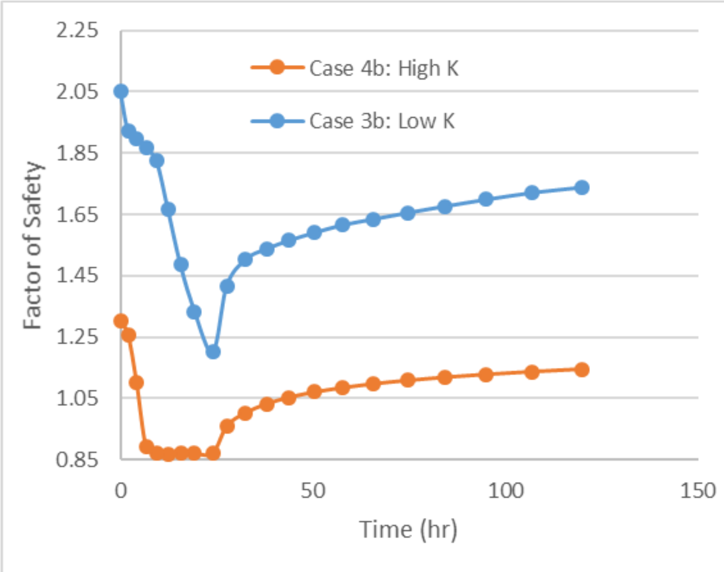

Figure 18. Comparison of FOS for a Rainfall Flux of 80 mm/hr using VWC Suction Strength.

Antecedent Moisture Conditions

The preceding analyses assumed that the initial pore-water pressure conditions were the same regardless of the material type. The short discussion in the Background section on infiltration into unsaturated soils clearly indicates that this would not be the case in the physical reality.

Figure 16 demonstrates that the high K and low K soils can support the annual infiltration flux of 1 m/year at matric suctions of about – 60 kPa and – 100 kPa, respectively. These values are observed in the simulated steady-state pore-water pressure profiles shown in Figure 19. The low K material generates more matric suction near the ground surface for the exact same infiltration flux and far-field boundary conditions as compared to the high K soil. In addition, the low K material produces a greater degree of mounding in the phreatic surface in order to transmit the vertical flux laterally to the edge of the domain. Mounding does not occur for the higher K soil. Correspondingly, the zero pressure value is located at a y-coordinate of about 15 m and 10 m for the low K and high K materials, respectively (Figure 19).

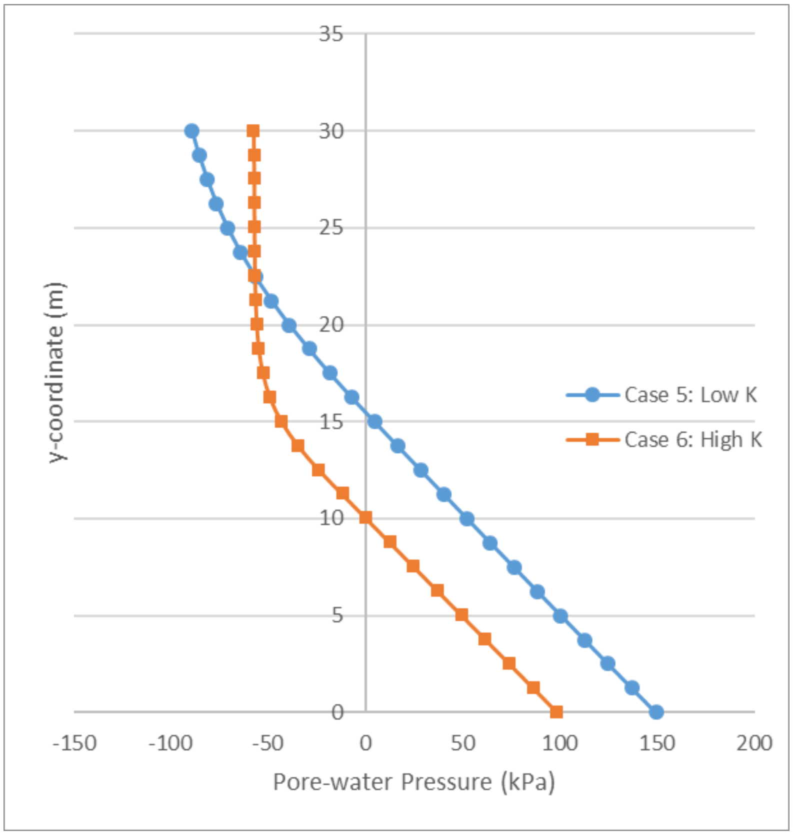

Figure 19. Pore-water pressure profiles for steady-state infiltration flux of 1 m/year.

Profiles of volumetric water content are shown in Figure 20. The antecedent moisture conditions are much wetter for the low K soil because the material can sustain higher water contents at larger matric suctions (Figure 6). Figure 21 and Figure 22 present the FOS for the low K and high K soil, respectively. The FOS for the low K soil is larger than that for the high K soil despite the mounding of the phreatic surface because of the higher suction strengths in the unsaturated zone.

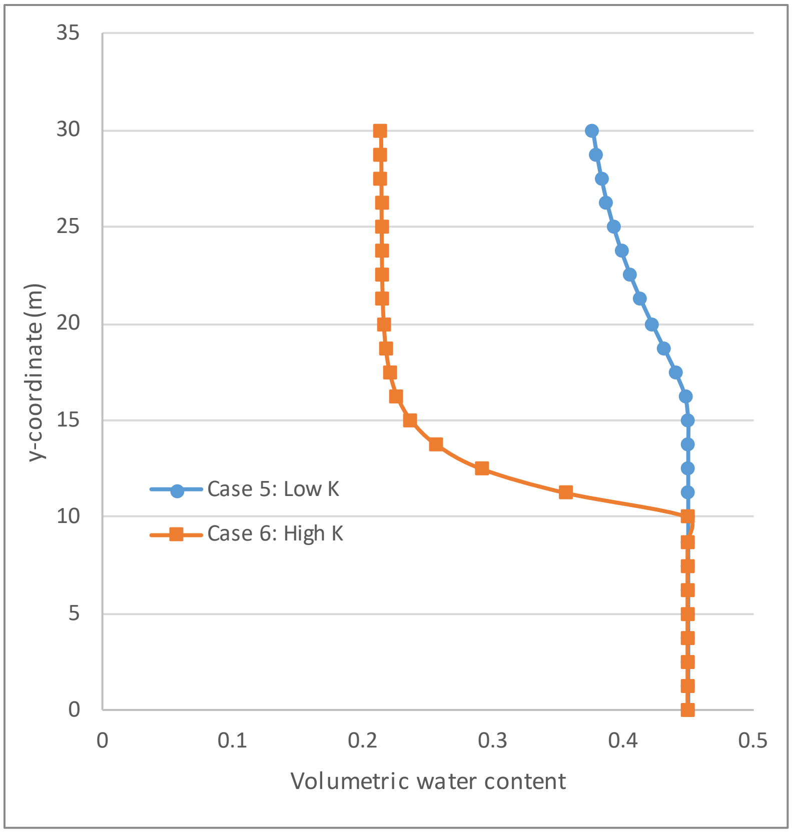

Figure 20. Volumetric water content profiles for an infiltration flux of 1 m/year.

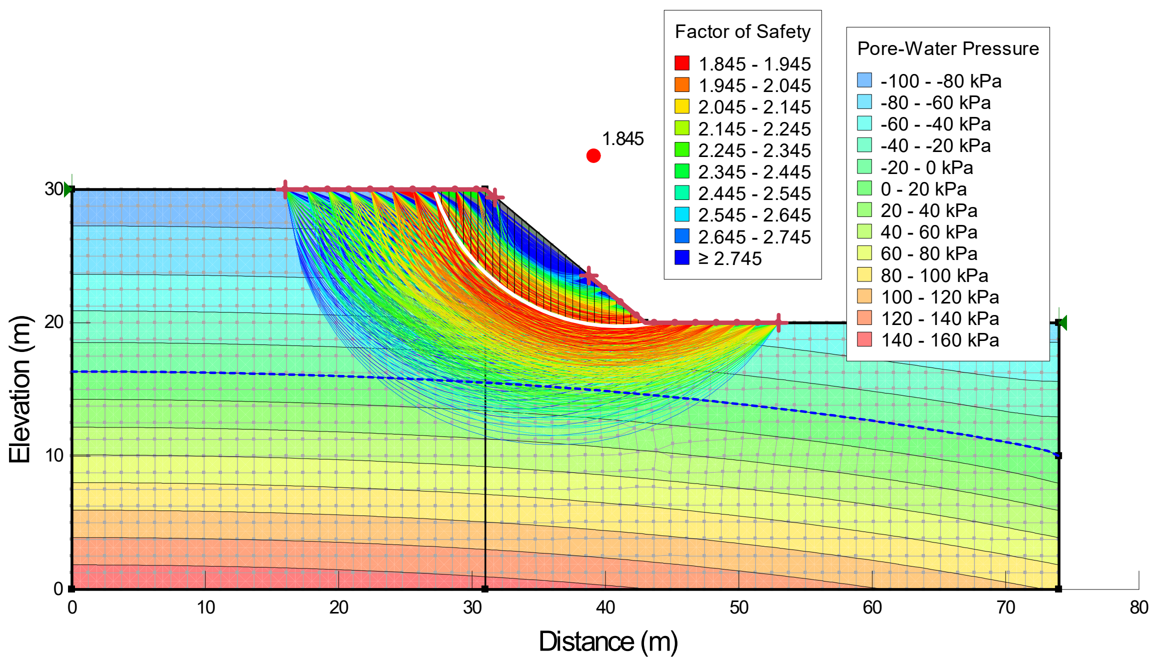

Figure 21. FOS for the lower K soil with a steady-state infiltration flux of 1 m/yr.

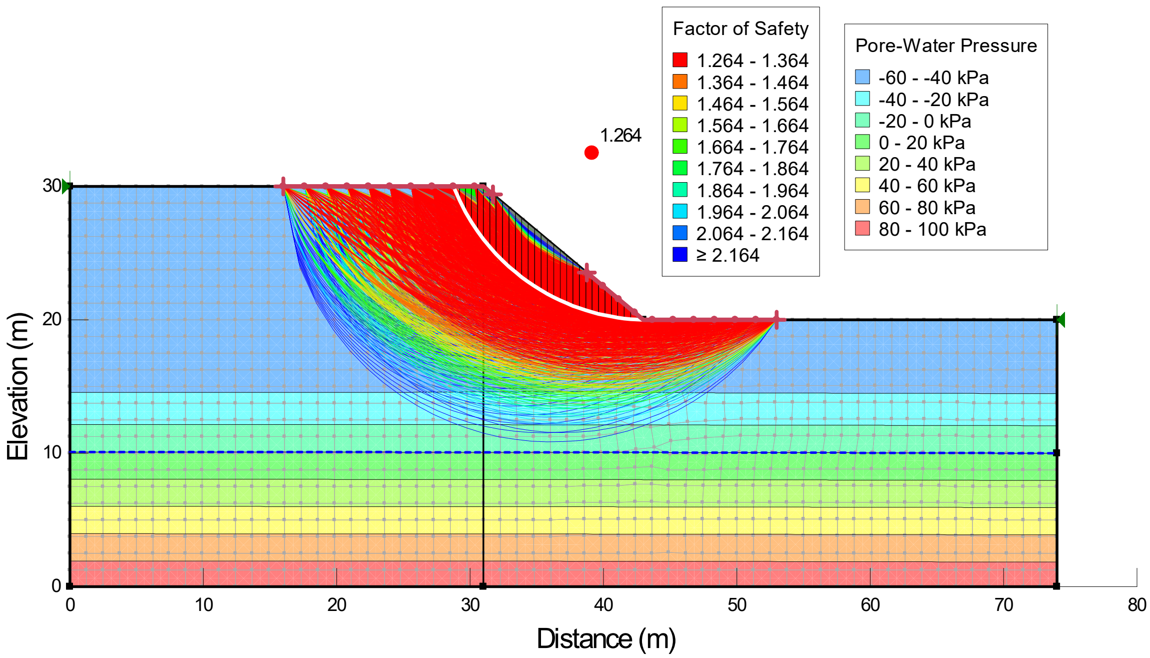

Figure 22. FOS for the high K soil with a steady-state infiltration flux of 1 m/yr.

Summary and Conclusions

The results of this parametric study confirmed that stability of homogeneous soil slopes depends on soil properties, infiltration flux, and antecedent moisture conditions. Rahardjo et al. (2007) noted that the saturated hydraulic conductivity and infiltration intensity impose the greatest control on stability, which is in-keeping with the results presented above. This study also demonstrated that the relative position of the hydraulic conductivity function relative to the infiltration flux is an important consideration. During infiltration, the pore-water pressure behind the wetting can be becomes constant. The magnitude of the pore-water pressure behind the wetting front depends on magnitude of the infiltration flux relative to the hydraulic conductivity function.

The results also demonstrated the importance of using a non-linear suction strength definition. The suction strength generated by a soil is closely linked to a materials ability to retain water at high matric suctions, as characterized by the volumetric water content function. There is generally an optimum water content range in which suction strengths can be significant. The use of a linear relationship does not reveal this important aspect of suction strength, even if careful consideration is given to the selection of ϕ^b.

The antecedent moisture conditions also impose a considerable control on the FOS prior to, and therefore during, a rainfall event. The initial matric suctions that develop in a soil profile are governed by the average annual rainfall flux relative to the hydraulic conductivity function for the soil. In systems with a deep unsaturated zone, the pore-water pressure profile is typically vertical, meaning that the hydraulic gradient is 1.0. The FOS will not necessarily be higher as the suction increases when a non-linear suction strength equation is considered. These equations normalize the strength based on the water content. The water content function is soil-dependent, so the antecedent moisture conditions will vary depending with soil type.

References

Anderson, S.A., and Zhu, J.H. 1996. Assessing the stability of a tropical residual slope. Proceedings, 7th International Symposium on Landslides, Rotterdam, The Netherlands, 1073-1077.

Kisch, M. 1959. The theory of seepage from clay-blanked reservoirs. Geotechnique. Vo. 9, 9-21.

Ng, C. W. W., Wang, B., and Tung, Y. K. 2001. Three-dimensional numerical investigations of groundwater responses in an unsaturated slope subjected to various rainfall patterns. Canadian Geotechnical Journal, Vol. 38, 1049–1062.

Rahardjo, H., Li, X.W., Toll, D.G., and Leong, E.C. 2001. The effect of antecedent rainfall on slope stability. Geotechnical and Geological Engineering, 19, 371-399.

Rahardjo, H., Ong, T.H., Rezaur, R.B., and Leong, E.C. 2007. Factors Controlling Instability of Homogeneous Soil Slopes under Rainfall. Journal of Geotechnical and Geoenvironmental Engineering, Vol. 133 (12), 1532 – 1543.

Tan, S.B., Tan, S.L., Lim, T.L., and Yang, K.S. 1987. Landslide problems and their control in Singapore. Proceedings, 9th Southeast Asian Geotechnical Conference, Vol. 1, Bangkok, Thailand, 25 -26.

Vanapalli, S.K., Fredlund, D.G., Pufhal, D.E. and Clifton, A.W. 1996. Model for the prediction of shear strength with respect to soil suction. Canadian Geotechnical Journal, Vol. 33 (3), 379 – 392.

Wong, H.N., and Ho, K.K.S. 1998. Systematic investigation of landslides caused by a severe rainstorm in Hong Kong. Transactions of the Hong Kong Institution of Engineers, Vol. 3 (3), 80.